frontiers | Frontiers in Environmental Science

TYPE Original Research
PUBLISHED 22 July 2022
DOI 10.3389/fenvs.2022.947924

OPEN ACCESS

EDITED BY
Yongjie Li,
University of Macau, China

REVIEWED BY
Masao Gen,
Tohoku University, Japan
Yangxi Chu,
Chinese Research Academy of Environmental Sciences, China

*CORRESPONDENCE
Mijung Song,
mijung.song@jbnu.ac.kr

SPECIALTY SECTION
This article was submitted to Atmosphere and Climate, a section of the journal Frontiers in Environmental Science

RECEIVED 19 May 2022
ACCEPTED 27 June 2022
PUBLISHED 22 July 2022

CITATION
Gaikwad S, Jeong R, Kim D, Lee K, Jang K-S, Kim C and Song M (2022), Microscopic observation of a liquid-liquid-(semi)solid phase in polluted $PM_{2.5}$.
Front. Environ. Sci. 10:947924.
doi: 10.3389/fenvs.2022.947924

Microscopic observation of a liquid-liquid-(semi)solid phase in polluted $PM_{2.5}$

Sanjit Gaikwad[1], Rani Jeong[1], Dohyun Kim[1], Kwangyul Lee[2], Kyoung-Soon Jang[3], Changhyuk Kim[4] and Mijung Song[1,5]*

[1]Department of Environment and Energy, Jeonbuk National University, Jeonju, South Korea, [2]Chungcheong Region Air Quality Research Center, Department of Air Quality Environment Research Division, Climate and Air Quality Research, National Institute of Environment Research, Seosan, South Korea, [3]Bio-Chemical Analysis Team, Korea Basic Science Institute, Cheongju, South Korea, [4]School of Civil and Environmental Engineering, Pusan National University, Busan, South Korea, [5]Department of Earth and Environmental Sciences, Jeonbuk National University, Jeonju, South Korea

Atmospheric aerosol particles are complex mixtures having various physicochemical properties. To predict the role and characteristics of such complex aerosol particles in air pollution and related atmospheric chemistry, our knowledge of the number and types of phases in complex aerosol particles should be improved. However, most studies on the phase behavior of aerosol particles have been conducted in the laboratory and have not used real-world aerosol particles. In this study, using a combination of optical microscopy and poke-and-flow technique, we investigated the number and types of phases of actual aerosol particles of particulate matter < 2.5 μm ($PM_{2.5}$) collected on heavily polluted days in Seosan, South Korea in winter 2020–2021. From the microscopic observations at 293 K, it showed that the $PM_{2.5}$ particles exist in a single liquid phase at relative humidity (RH) >~85%, a liquid-liquid phase at ~70% < RH <~85%, a liquid-liquid-(semi)solid phase at ~30% < RH <~70%, and a (semi)solid phase at RH <~30% upon dehydration. This reveals that three phases of atmospheric aerosol particles coexisting as liquid-liquid and liquid-liquid-(semi)solid would be the most common phases in the atmosphere considering ambient RH ranges. These observations provide fundamental properties necessary for improved predictions of air quality and aerosol chemistry such as reactive uptake of N_2O_5, size distributions, and mass concentrations of aerosol particles.

KEYWORDS

liquid-liquid-(semi)solid, phase state, phase behavior, $PM_{2.5}$, aerosol pollution

Introduction

Particulate matter (PM) is a ubiquitous component of the atmosphere. PM is emitted from primary sources and can also be generated by secondary formation owing to chemical reactions in the atmosphere (Seinfeld and Pandis, 2016). PM, especially $PM_{2.5}$, can significantly affect ecosystems, climate, and human health (Peng et al., 2016; Wang et al., 2016; Bhattarai et al., 2020). In Asia, $PM_{2.5}$ pollution has become a serious

environmental issue over the past few decades (Pörtner et al., 2019; Ting et al., 2022). Numerous field measurements have shown that $PM_{2.5}$ mainly comprises organic materials and inorganic salts (Jimenez et al., 2009; Zhang et al., 2017) and are often internally mixed in $PM_{2.5}$ in various environments (Vester et al., 2007; Ye et al., 2018).

To understand the impacts of $PM_{2.5}$ on atmospheric chemistry and air quality, information on the physical properties of the phase types (i.e., liquid, semisolid, or solid) and number of phases (i.e., one, two, or three phases) of atmospheric aerosol particles is essential. The phase states of particles are a crucial part of aerosol growth and evaporation, mass concentration of aerosol particles (Shiraiwa and Seinfeld, 2012; Yli-Juuti et al., 2017), ice nucleation efficiency (Ladino et al., 2014; Knopf et al., 2018), crystallinity of salts (Ji et al., 2017; Wang et al., 2017), and heterogeneous reactivity (Li et al., 2020; Xu et al., 2020). Many laboratory experiments and modelling studies have been performed to explore the phases of atmospheric aerosol particles (Virtanen et al., 2010; Koop et al., 2011; Renbaum-Wolff et al., 2013; Song et al., 2015; Reid et al., 2018; Riemer et al., 2019; Lilek and Zuend, 2022). Most laboratory studies on phase states have focused on pure secondary organic aerosols (SOA) as a function of relative humidity (RH) (Koop et al., 2011; Song et al., 2015; Athanasiadis et al., 2016; Song et al., 2016; Schmedding et al., 2020). These studies have reported that SOA particles range from liquid to semisolid or solid depending on the RH. Moreover, a recent study investigated SOA mixed with inorganic salts, and showed a sudden change in their phase state at a certain RH close to efflorescence RH as the inorganic fraction increased (Song et al., 2021; Jeong et al., 2022).

Mixtures of SOA and inorganic salts have also been investigated to determine the number of phases and their corresponding morphologies (Krieger et al., 2012; Song et al., 2012a; You et al., 2014; Freedman, 2017). In internally mixed organic/inorganic salt aerosol particles, two liquid phases by liquid-liquid phase separation are always observed over a wide range of RH when the oxygen-to-carbon ratio (O:C) is lower than 0.56 (Bertram et al., 2011; Song et al., 2012a; Song et al., 2012b; Song et al., 2013). Interestingly, recent studies have reported three liquid phases in organic/inorganic aerosol particles (Kucinski et al., 2019; Huang et al., 2021). Moreover, liquid-liquid phase separation has also been observed in some types of SOA particles free of inorganic salts (Renbaum-Wolff et al., 2016; Song et al., 2017; Ham et al., 2019). To date, most of the types and number of phases have been investigated based on laboratory studies as it is challenging to directly monitor the types and number of phases of real atmospheric aerosol particles using online instruments, and very few instruments are available to analyze such properties.

Several studies have been conducted on the types and number of phases using ambient PM with complex chemical compositions. Pöhlker et al. (2012) and You et al. (2012) analyzed liquid–liquid phase separation in total suspended particulates collected from clean areas in the Amazonian rainforest and central Atlanta, respectively. Virtanen et al. (2010) observed an amorphous solid phase of atmospheric PM in a boreal forest environment under low RH conditions in Hyytiälä, Finland. In contrast, Pajunoja et al. (2016) observed mostly organic ambient particles in a liquid phase over the southeastern United States. Bateman et al. (2017) showed that submicron PM was in a liquid phase at RH >80%, while non-liquid behavior was observed at RH <60% in central Amazonia. Liu et al. (2017) showed a more liquid-like behavior with an increase in the inorganic fraction in submicron PM during a haze episode in Beijing. Although the physical properties of aerosol particles are key parameters for predicting heterogeneous reactions and particle size distributions (Shiraiwa et al., 2013; Su et al., 2020), our understanding of the phase behavior of real aerosol particles is far from complete.

To obtain further insights on the phase behavior of real-world aerosol particles, we collected seven $PM_{2.5}$ samples at Seosan, South Korea, during December 26 – 29, 2020, and January 11–13, 2021. The atmosphere in and around Seosan is heavily influenced by agricultural and anthropogenic emissions (Ju et al., 2020; Hwang et al., 2021). Inorganic salts and water-soluble organic material were extracted in pure water from the $PM_{2.5}$ filters. Using the $PM_{2.5}$ droplets at 293 ± 1 K, we determined the types and number of phases upon dehydration by microscopic observations combined with the poke-and-flow technique.

Experimental

Site description

Measurements were carried out at the Chungcheong Air Environment Research Center, Seosan, Chungcheongnam-do, Republic of Korea (126.494°E, 36.777°N), during December 26–29, 2020, and January 11–13, 2021 (Figure 1). Seosan is a rural area, where the air quality is heavily influenced by both agricultural and anthropogenic emissions (Ju et al., 2020; Hwang et al., 2021). It is surrounded by an agricultural cluster, a petrochemical complex is located 26 km to the northwest, and thermal power plants (10 units) are located ~27 km to the northwest (Lee et al., 2017; Ju et al., 2020). The total land area of Seosan city is 743.9 km^2 and it has a population of 176,379 with a population density of 237.1 people/km^2 of land area (Ju et al., 2020).

Collection and production of $PM_{2.5}$

$PM_{2.5}$ was collected on quartz filters for 23 h (10:00 a.m. – 09:00 a.m.) using a high-volume air sampler (SIBATA, HV-

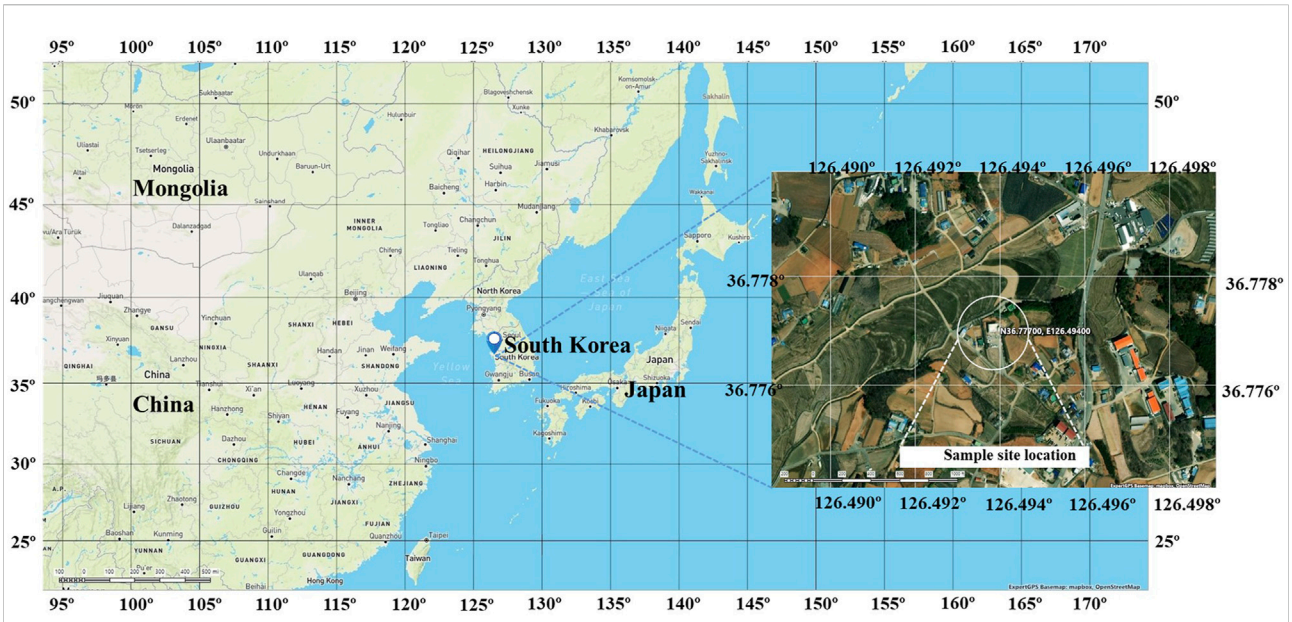

FIGURE 1
Location of a sampling site at rural area, Seosan.

1000R, Japan) on the rooftop of the monitoring site, ~10 m above the ground level. After collection, the filter samples were stored in a freezer (−18°C) until further analysis. We analyzed $PM_{2.5}$ particles from the filter samples to explore the phase behavior of $PM_{2.5}$. The inorganic salts and water-soluble organic material on the $PM_{2.5}$ filters were extracted in purified water (18.2 MΩ cm, Merck Milli-Q®, Millipore, Burlington, MA, United States) within 1 month of collection. The extracts were then nebulized using a nebulizer (MEINHARD®, United States) onto a hydrophobic substrate to produce micrometer-sized particles, which were used for optical observations at 293 ± 1 K.

Optical microscopy of $PM_{2.5}$ single droplets

The $PM_{2.5}$ extracts on a hydrophobic glass slide were placed in a temperature- and RH-controlled flow-cell (Song et al., 2012a; Ham et al., 2019). At the beginning of the experiment, the $PM_{2.5}$ droplets in the cell were equilibrated at ~100% RH for ~20 min. RH was then decreased at a rate of ~0.5% RH/min. During the experiment, the morphological changes in the droplets were monitored using an optical microscope (Olympus BX43, 40× objective, Japan) and recorded every 5 s using a charge-coupled device camera (DigiRetina 16, Tucsen, China). The RH in the cell was controlled by the N_2 and H_2O ratio, with a total flow rate of 500 sccm. The RH was calibrated by measuring the deliquescence RH of K_2CO_3 (44% RH) and NaCl (76% RH) at 293 ± 1 K, leading to an RH uncertainty of ± 1.5% (Winston and Bates, 1960).

Poke-and-flow technique for single droplets

The poke-and-flow experiment (Murray et al., 2012; Renbaum-Wolff et al., 2013) was performed to determine the semisolid or solid [herein, we refer to semisolid or solid as "(semi)solid"] phase state of $PM_{2.5}$, based on a previously reported procedure (Renbaum-Wolff et al., 2013; Grayson et al., 2016; Song et al., 2019; Jeong et al., 2022). In this study, the experimental flow time, which is the recovery time of the inner hole of a particle after poking, could not be determined because the $PM_{2.5}$ droplets were supersaturated with inorganic salts upon dehydration. Therefore, we attempted to determine the RH at which the particles cracked using a sharp sterile needle (Jung Rim Medical Industrial, South Korea) upon dehydration. The droplets on the hydrophobic substrate were conditioned at a target RH for ~2 h into an RH-controlled flow-cell after conditioning at an RH of ~100%. The droplets were then poked, and the particles were observed for ~3 h to check whether inflow or outflow occurred. If no flow was observed, we defined the particle as (semi)solid based on previous studies (Renbaum-Wolff et al., 2013; Grayson et al., 2016; Song et al., 2019;

TABLE 1 Summary of the chemical compositions, oxygen-to-carbon elemental ratio (O:C), and relative humidity (RH) in liquid-liquid, liquid-liquid-(semi)solid, and (semi)solid phase states of $PM_{2.5}$ with decreasing RH based on the interval of filter sampling.

Date	$PM_{2.5}$ (μg/m^3)	NO_3^- (μg/m^3)	NH_4^+ (μg/m^3)	SO_4^{2-} (μg/m^3)	OC (μg/m^3)	EC (μg/m^3)	O:C	RH liquid-liquid (%)	RH liquid-liquid-(semi)solid (%)	RH (semi) solid (%)
20.12.26	47.7 ± 12.9	11.1 ± 5.2	4.8 ± 1.8	2.8 ± 0.8	7.6 ± 3.4	1.9 ± 1.1	0.41 ± 0.1	83 ± 2.1	68.0 ± 2.3	22.0 ± 2.0
20.12.27	32.4 ± 7.2	5.8 ± 1.1	2.9 ± 0.6	2.4 ± 0.4	5.1 ± 2.4	1.4 ± 0.6	0.38 ± 0.2	84 ± 2.3	57.4 ± 2.0	30.0 ± 2.0
20.12.28	54.2 ± 9.9	13.0 ± 5.4	5.9 ± 2.2	4.5 ± 1.6	6.3 ± 1.8	1.9 ± 0.3	0.41 ± 0.1	81 ± 1.8	63.8 ± 2.5	20.0 ± 2.5
20.12.29	40.5 ± 13.0	7.7 ± 3.8	3.6 ± 1.9	3.9 ± 1.4	4.7 ± 1.1	1.1 ± 0.1	0.40 ± 0.1	82 ± 1.5	71.2 ± 2.6	20.0 ± 2.0
21.01.11	46.6 ± 11.0	8.7 ± 2.1	4.4 ± 0.8	3.5 ± 0.4	7.4 ± 3.5	2.1 ± 0.7	0.41 ± 0.1	80 ± 1.7	69.3 ± 2.2	22.0 ± 2.2
21.01.12	45.8 ± 9.4	9.0 ± 3.6	4.6 ± 1.9	4.0 ± 1.3	6.2 ± 4.1	1.9 ± 0.7	0.40 ± 0.1	81 ± 2.2	67.5 ± 2.6	23.0 ± 2.0
21.01.13	44.0 ± 7.9	6.1 ± 1.7	2.7 ± 0.6	2.4 ± 0.3	4.8 ± 1.6	1.5 ± 0.7	0.41 ± 0.1	81 ± 2.1	74.3 ± 2.5	13.0 ± 2.3

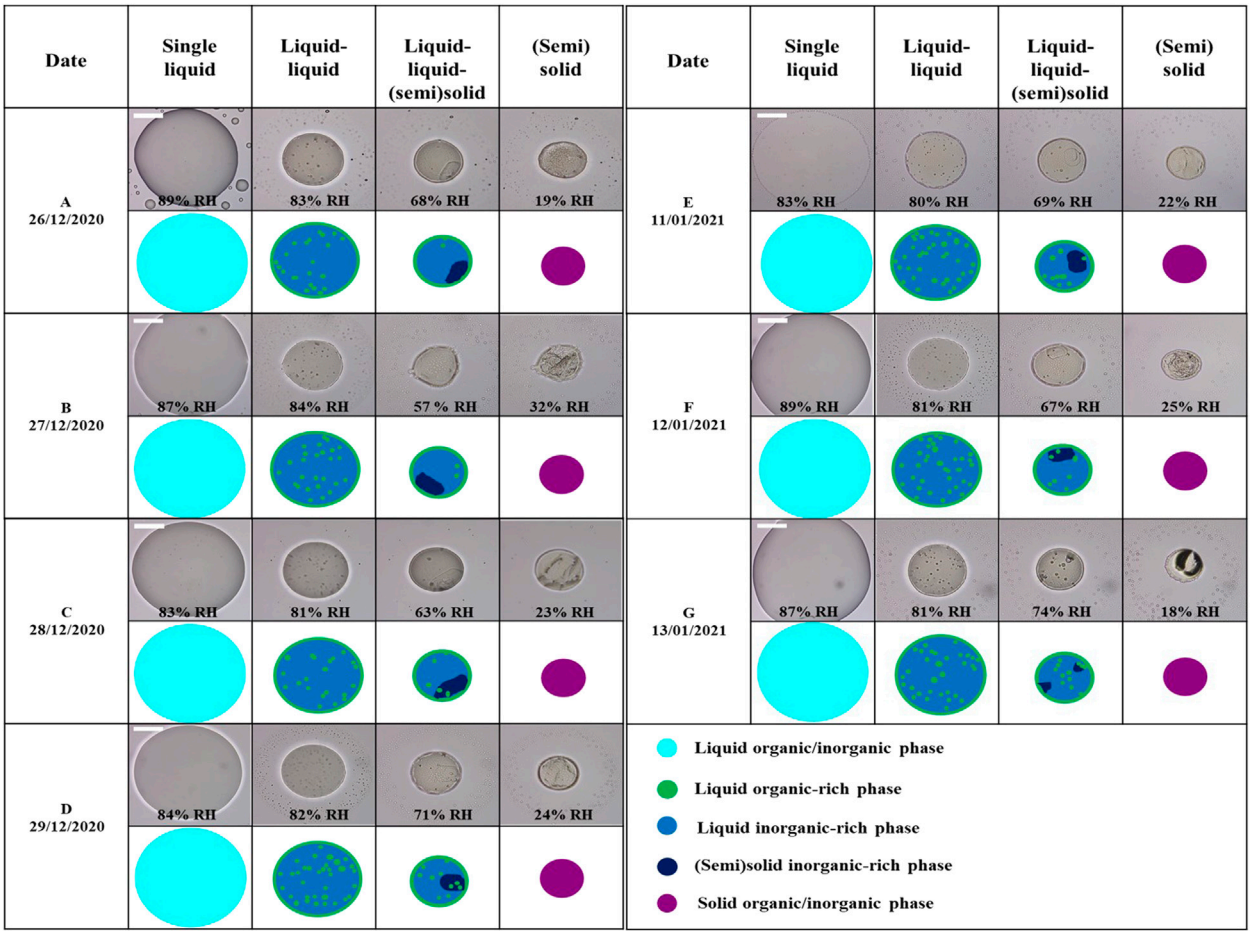

FIGURE 2
Optical images of $PM_{2.5}$ filter samples collected in winter at Seosan, South Korea, and its cartoon with decreasing RH at ~293 K. The Second, third, and fourth columns represent the single liquid, liquid-liquid, and liquid-liquid-(semi)solid phase states of $PM_{2.5}$, respectively. The fifth columns represent a (semi)solid phase state showing efflorescence over the particles. The scale bar is 20 μm. In the illustration, cyan color: liquid organic/inorganic phase, green color: liquid organic-rich phase, blue color: liquid inorganic-rich phase, dark blue color: semi(solid) inorganic-rich phase, and purple color: (semi)solid organic/inorganic.

Jeong et al., 2022). During the poke-and-flow experiments, the particles were observed before, during, and after they were poked with a needle using an optical microscope (Olympus CKX53 with a 40× objective, Japan) and recorded using a charge-coupled device camera (Hamamatsu, C11440-42U30, Japan).

Chemical composition of $PM_{2.5}$

Raman spectroscopy (XploRA PLUS, HORIBA, France) coupled with an optical microscope was used to identify the main chemical compositions of liquid-liquid phase-separated $PM_{2.5}$ droplets. An Nd:YAG laser (532 nm wavelength) was used as the excitation source. A grating with 1,800 grooves mm^{-1} and an acquisition time of 5 s with an accumulation of 20 grooves was used. The Raman spectra at different positions of the inner and outer phases of $PM_{2.5}$ droplets were recorded in the range of 150–4,000 cm^{-1}.

The oxygen-to-carbon elemental ratio (O:C) of WSOC fraction in $PM_{2.5}$ sample was estimated from molecular formulas identified by Fourier transform ion cyclotron resonance mass spectrometer, as previously demonstrated (Choi et al., 2017). The chemical compositions and meteorological parameter were reported in Kim et al. (2022) and, in this study, we analyzed the data based on the interval of the filter sampling.

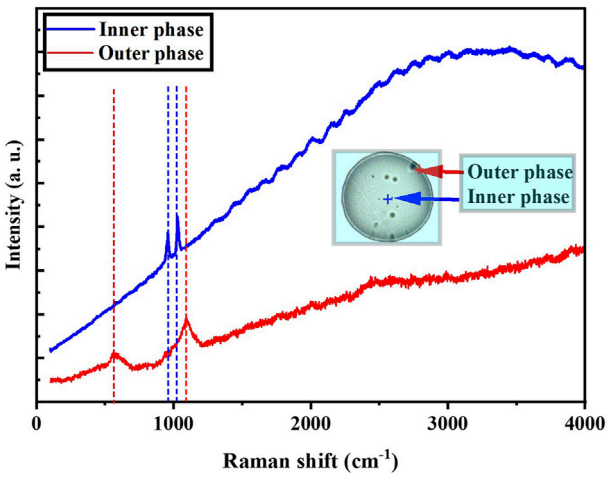

FIGURE 3
Raman spectra of liquid-liquid phase-separated $PM_{2.5}$ particle collected in 28 December 2020 at relative humidity of 80%. Blue dash lines represent the inorganic peaks while the red dash lines represent the organic peaks.

Results and discussion

To determine the phase behavior of real aerosol particles, we collected seven different $PM_{2.5}$ samples during winter in a rural area, Seosan, in South Korea. It has been reported that severe $PM_{2.5}$ pollution occurs frequently in this area (Ju et al., 2020; Hwang et al., 2021; Park et al., 2022). During the sampling period, all seven samples indicated $PM_{2.5}$ pollution based on the guideline value of 15 $\mu g/m^3$ for 24-h mean $PM_{2.5}$, according to the World Health Organization (2021). Information on the chemical compositions and meteorological parameters of $PM_{2.5}$ samples is summarized in Table 1.

Figure 2 shows the optical images and corresponding illustrations of each polluted $PM_{2.5}$ sample as the RH decreased at 293 K. The phase changes in the optical images of each $PM_{2.5}$ droplets are also shown in Supplementary Movies S1–S7. Initially, $PM_{2.5}$ was maintained at ~100% RH for 20 min and the droplets exhibited a single liquid phase. With decreasing RH, the size of the droplets decreased because of the evaporation of water. The second column in Figure 2 represents the single liquid phase of each $PM_{2.5}$ sample collected on different dates for the RH at which the droplets did not undergo any phase transitions during the decrease in RH. At ~85% RH upon dehydration, all $PM_{2.5}$ droplets underwent liquid-liquid phase separation and formed a core-shell morphology with some inclusions in the inner phase. Laboratory studies have established that liquid-liquid phase separation always occurs for O:C < 0.56 in organic/inorganic aerosol particles (Bertram et al., 2011; Song et al., 2012b). In the current study, the O:C of the $PM_{2.5}$ ranged from 0.38 to 0.41 (Table 1). These values are within the range of occurrence of liquid-liquid phase separation. You et al. (2012) and Pöhlker et al. (2012) also observed liquid-liquid phase separation in total suspended particles within these O:C ratios, which were established from laboratory studies in clean environments in Atlanta and near Amazon, respectively.

In the phase-separated $PM_{2.5}$ droplets, small satellite inclusions were observed in the inner phase as shown in third columns of Figure 2. Such small satellite inclusions were also observed in outer phase when phase separation occurred in organic/inorganic/H_2O particles, and then they were disappeared as RH decreased (Ciobanu et al., 2009; Song et al., 2012a). Although we could not access to determine the chemical compositions using the tiny satellite inclusions of the $PM_{2.5}$ in this study, we observed during decreasing RH that the tiny satellite inclusions appeared when the phase separation occurred and then disappeared as RH decreased further. This behavior of the satellite inclusions is very similar to the behavior observed in the organic/inorganic/H_2O particles. Thus, we expect that the satellite inclusions observed in the inner phase of the $PM_{2.5}$ droplet are most likely organic compounds.

We analyzed the chemical compositions of the inner and outer phases of a phase-separated $PM_{2.5}$ droplet at ~80% RH collected in 28 December 2020. Raman spectra from the inner phase of the droplet showed two sharp peaks at ~971 cm^{-1} and ~1,030 cm^{-1} belonging to SO_4^{2-} and NO_3^-, respectively (Cheng et al., 2021) (blue line in Figure 3). Two distinct peaks were also observed from the outer phase of the droplet at 1,096 cm^{-1}, relevant to the vibrational mode of organic functional group ν(C–O) (Bondy et al., 2018), and at 576 cm^{-1} due to the carboxyl vibration (Eshelman et al., 2014) (red line in Figure 3). This result reveals that the core consists mainly of inorganic salts surrounded by organic materials in the liquid-liquid phase-

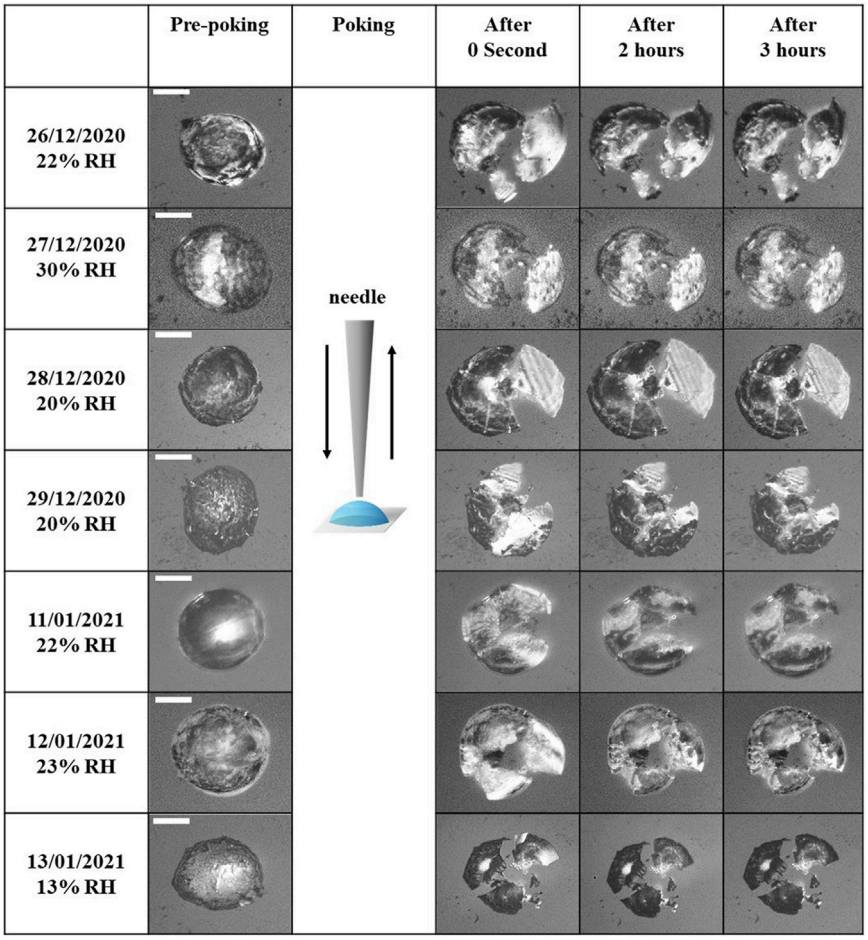

FIGURE 4
Optical images of pre-poking, poking, and post-poking for polluted $PM_{2.5}$ filter samples during the poke-and-flow experiment. The scale bar is 10 μm.

separated particles. This is consistent with previous work (Song et al., 2012b).

Interestingly, as RH decreased, a crystal suddenly appeared in the liquid inner phase of each $PM_{2.5}$ sample, leading to three coexisting phases at RH between ~70% and ~30%, as shown in forth columns of Figure 2 (also Supplementary Movies S1–S7). This result is the first such observation of the phase behavior of real aerosol particles of $PM_{2.5}$, with three phases coexisting a liquid-liquid-(semi)solid. Based on the shape and morphology of the crystal in the inner liquid phase, these were assumed to be (semi)solid inorganic salts such as ammonium nitrate, ammonium sulfate, or sodium chloride (Ebert and Weinbruch, 2001; Zelenyuk et al., 2006; Furstenberg et al., 2010). A recent study by Huang et al. (2021) observed the existence of three phases with liquid-liquid-liquid for ~40% – ~90% RH in a mixture of SOA, primary organic aerosols, and secondary inorganic aerosols. This is a contrast with our observation that three phases with a liquid-liquid-(semi)solid in the $PM_{2.5}$ were coexisted for RH of ~30% – ~70%. These three phases of the droplets coexisted until the droplets effloresced over the particle (i.e., ~30% RH, Figure 2).

A further decrease in RH led to efflorescence of the droplets (last columns of Figure 2). However, at this stage, it was not clear based on the optical image whether the droplets fully or partially effloresced so that the phase state became (semi)solid or still liquid-like over the total particle. Thus, we applied another technique using the poke-and-flow to define the phase with the same procedure of a recent study of Jeong et al. (2022) that determined the phase of particles of organic/inorganic mixtures. Figure 4 shows the poke-and-flow result for the seven different $PM_{2.5}$ particles. On pre-poking, effloresced particles were present, and the particles started to crack at RH <~30% after being poked with the needle. Subsequently, no restorative flow was detected for approximately 3 h. This produces viscosities of greater than ~10^8 Pa s corresponding to a semisolid or a solid phase state (Renbaum-Wolff et al., 2013;

Grayson et al., 2016; Song et al., 2019; Jeong et al., 2022). Additionally, we tried to poke the particles at an RH ~10% higher than the RH at which they cracked, but the particles were stuck to the needle. Based on the procedure, the point at which all $PM_{2.5}$ particles cracked was determined as (semi)solid phase (Table 1). The RH values of efflorescence (fourth column of Figure 2) and particle cracked (Figure 4) are similar within experimental errors. The overall results showed that the $PM_{2.5}$ exhibited a single liquid phase at RH >~85%, liquid-liquid phase at ~70% < RH < ~85%, liquid-liquid-(semi)solid phase at ~30% < RH < ~70%, and a (semi)solid phase at RH < ~30%. This result indicates that phases coexisting a liquid-liquid or a liquid-liquid-(semi)solid of aerosol particles would be the most common phases in the atmosphere considering ambient RH distributions (Song et al., 2019).

This study provides observational evidence for the phase behavior of real aerosol particles. The existence of three phases consisting of a liquid-liquid-(semi)solid (outer phase is mainly liquid organic-rich) has implications for the uptake rate of reactive gases into particles. Studies have shown that N_2O_5 reacts with inorganic-rich droplets, which leads to increased concentrations of particulate nitrate (Dentener and Crutzen, 1993; Riemer et al., 2009; Huang et al., 2021). However, recent studies have shown that organic coating in a droplet can lead to reactions on the surface area resulting in the reduction of the reactive uptake of N_2O_5 (Folkers et al., 2003). The uptake rate of a particle can be varied based on the polarity of the organic phase (Huang et al., 2021). Furthermore, studies have shown that other trace reactive gases such as amines exhibited a lower tendency towards heterogeneous uptake by organic-coated particles (Chu and Chan, 2017; Sauerwein and Chan, 2017). Further studies are thus required to confirm our results with different conditions (i.e., various environments and temperature) and to extend the phase effects on heterogeneous reactions.

Data availability statement

The original contributions presented in the study are included in the article/Supplementary Material, further inquiries can be directed to the corresponding author.

Author contributions

MS designed this study. All authors conducted measurements and analyzed the data. MS and SG prepared the manuscript with the contributions of all co-authors. All authors have read and agreed to the published version of the manuscript.

Funding

This work was supported by the Fine Particle Research Initiative in East Asia Considering National Differences (FRIEND) Project (NRF-2020M3G1A1114548), and by the National Research Foundation of Korea (NRF) grant funded by the Korean government (MSIT) (NRF-2019R1A2C1086187).

Conflict of interest

The authors declare that the research was conducted in the absence of any commercial or financial relationships that could be construed as a potential conflict of interest.

Publisher's note

All claims expressed in this article are solely those of the authors and do not necessarily represent those of their affiliated organizations, or those of the publisher, the editors and the reviewers. Any product that may be evaluated in this article, or claim that may be made by its manufacturer, is not guaranteed or endorsed by the publisher.

Supplementary material

The Supplementary Material for this article can be found online at: https://www.frontiersin.org/articles/10.3389/fenvs.2022.947924/full#supplementary-material

References

Athanasiadis, A., Fitzgerald, C., Davidson, N. M., Giorio, C., Botchway, S. W., Ward, A. D., et al. (2016). Dynamic viscosity mapping of the oxidation of squalene aerosol particles. *Phys. Chem. Chem. Phys.* 18 (44), 30385–30393. doi:10.1039/c6cp05674a

Bateman, A. P., Gong, Z. H., Harder, T. H., de Sá, S. S., Wang, B. B., Castillo, P., et al. (2017). Anthropogenic influences on the physical state of submicron particulate matter over a tropical forest. *Atmos. Chem. Phys.* 17 (3), 1759–1773. doi:10.5194/acp-17-1759-2017

Bertram, A. K., Martin, S. T., Hanna, S. J., Smith, M. L., Bodsworth, A., Chen, Q., et al. (2011). Predicting the relative humidities of liquid-liquid phase separation, efflorescence, and deliquescence of mixed particles of ammonium sulfate, organic material, and water using the organic-to-sulfate mass ratio of the particle and the oxygen-to-carbon elemental ratio of the organic component. *Atmos. Chem. Phys.* 11 (21), 10995–11006. doi:10.5194/acp-11-10995-2011

Bhattarai, G., Lee, J. B., Kim, M. H., Ham, S., So, H. S., Oh, S., et al. (2020). Maternal exposure to fine particulate matter during pregnancy induces progressive senescence of hematopoietic stem cells under preferential impairment of the bone marrow microenvironment and aids development of myeloproliferative disease. *Leukemia* 34 (5), 1481–1484. doi:10.1038/s41375-019-0665-8

Bondy, A. L., Craig, R. L., Zhang, Z., Gold, A., Surratt, J. D., Ault, A. P., et al. (2018). Isoprene-Derived organosulfates: Vibrational mode analysis by Raman spectroscopy, acidity-dependent spectral modes, and observation in individual

atmospheric particles. *J. Phys. Chem. A* 122 (1), 303–315. doi:10.1021/acs.jpca.7b10587

Cheng, H. Y., Dong, X., Yang, Y., Feng, Y. Q., Wang, T., Tahir, M. A., et al. (2021). Au nanoring arrays as surface enhanced Raman spectroscopy substrate for chemical component study of individual atmospheric aerosol particle. *J. Environ. Sci.* 100, 11–17. doi:10.1016/j.jes.2020.07.003

Choi, J. H., Ryu, J., Jeon, S., Seo, J., Yang, Y. H., Pack, S. P., et al. (2017). In-depth compositional analysis of water-soluble and -insoluble organic substances in fine ($PM_{2.5}$) airborne particles using ultra-high resolution 15T FT-ICR MS and GCx GC-TOFMS. *Environ. Pollut.* 225, 329–337. doi:10.1016/j.envpol.2017.02.058

Chu, Y., and Chan, C. K. (2017). Role of oleic acid coating in the heterogeneous uptake of dimethylamine by ammonium sulfate particles. *Aerosol Sci. Technol.* 51 (8), 988–997. doi:10.1080/02786826.2017.1323072

Ciobanu, V. G., Marcolli, C., Krieger, U. K., Weers, U., and Peter, T. (2009). Liquid– liquid phase separation in mixed organic/inorganic aerosol particles. *J. Phys. Chem. A* 113 (41), 10966–10978. doi:10.1021/jp905054d

Dentener, F. J., and Crutzen, P. J. (1993). Reaction of N_2O_5 on tropospheric aerosols: Impact on the global distributions of NO_x, O_3, and OH. *J. Geophys. Res.* 98 (D4), 7149–7163. doi:10.1029/92jd02979

Ebert, M., and Weinbruch, S. (2001). High-resolution scanning electron microscopy of atmospheric particles sampled at Jungfraujoch during the CLACE field experiment. *High Alt. Res. Stn. Gornergrat.* 57, 57–62.

Eshelman, E., Daly, M. G., Slater, G., Dietrich, P., and Gravel, J. F. (2014). An ultraviolet Raman wavelength for the *in-situ* analysis of organic compounds relevant to astrobiology. *Planet. Space Sci.* 93-94, 65–70. doi:10.1016/j.pss.2014.01.021

Folkers, M., Mentel, T. F., and Wahner, A. (2003). Influence of an organic coating on the reactivity of aqueous aerosols probed by the heterogeneous hydrolysis of N_2O_5. *Geophys. Res. Lett.* 30 (12), 1644. doi:10.1029/2003gl017168

Freedman, M. A. (2017). Phase separation in organic aerosol. *Chem. Soc. Rev.* 46 (24), 7694–7705. doi:10.1039/c6cs00783j

Furstenberg, R., Papantonakis, M., Kendziora, C., Bubb, D., Corgan, J., and McGill, R. A. (2010). Laser vaporization of trace explosives for enhanced non-contact detection. *SPIE* 7665, 205–216. doi:10.1117/12.850385

Grayson, J. W., Zhang, Y., Mutzel, A., Renbaum-Wolff, L., Böge, O., Kamal, S., et al. (2016). Effect of varying experimental conditions on the viscosity of α-pinene derived secondary organic material. *Atmos. Chem. Phys.* 16 (10), 6027–6040. doi:10.5194/acp-16-6027-2016

Ham, S., Babar, Z. B., Lee, J. B., Lim, H.-J., and Song, M. (2019). Liquid–liquid phase separation in secondary organic aerosol particles produced from α-pinene ozonolysis and α-pinene photooxidation with/without ammonia. *Atmos. Chem. Phys.* 19 (14), 9321–9331. doi:10.5194/acp-19-9321-2019

Huang, Y., Mahrt, F., Xu, S., Shiraiwa, M., Zuend, A., Bertram, A. K., et al. (2021). Coexistence of three liquid phases in individual atmospheric aerosol particles. *Proc. Natl. Acad. Sci. U. S. A.* 118 (16), e2102512118. doi:10.1073/pnas.2102512118

Hwang, K.-W., Kim, J., and Kwon, Y.-J. (2021). A study on the factors affecting the air environment in chungnam province-focusing on cheonan, dangjin, and seosan. *J. Korea. Acad. Indust. Coop. Soc.* 22 (5), 118–127. doi:10.5762/KAIS.2021.22.5.118

Jeong, R., Lilek, J., Zuend, A., Xu, R., Chan, M. N., Kim, D., et al. (2022). Viscosity and physical state of sucrose mixed with ammonium sulfate droplets. *Atmos. Chem. Phys. Discuss.*, 1–21. doi:10.5194/acp-2022-74

Ji, Z. R., Zhang, Y., Pang, S. F., and Zhang, Y. H. (2017). Crystal nucleation and crystal growth and mass transfer in internally mixed sucrose/$NaNO_3$ particles. *J. Phys. Chem. A* 121 (41), 7968–7975. doi:10.1021/acs.jpca.7b08004

Jimenez, J. L., Canagaratna, M. R., Donahue, N. M., Prevot, A. S., Zhang, Q., Kroll, J. H., et al. (2009). Evolution of organic aerosols in the atmosphere. *Science* 326 (5959), 1525–1529. doi:10.1126/science.1180353

Ju, S., Yu, G. H., Park, S., Lee, J., Lee, S., Jee, J., et al. (2020). Pollution characteristics of $PM_{2.5}$ measured during fall at a seosan site in Chungcheong province. *J. Korean Soc. Atmos. Environ.* 36 (3), 329–345. doi:10.5572/Kosae.2020.36.3.329

Kim, N. K., Kim, Y. P., Ghim, Y. S., Song, M. J., Kim, C. H., Jang, K. S., et al. (2022). Spatial distribution of $PM_{2.5}$ chemical components during winter at five sites in Northeast Asia: High temporal resolution measurement study. *Atmos. Environ.* submitted.

Knopf, D. A., Alpert, P. A., and Wang, B. B. (2018). The role of organic aerosol in atmospheric ice nucleation: A review. *ACS Earth Space Chem.* 2 (3), 168–202. doi:10.1021/acsearthspacechem.7b00120

Koop, T., Bookhold, J., Shiraiwa, M., and Poschl, U. (2011). Glass transition and phase state of organic compounds: dependency on molecular properties and implications for secondary organic aerosols in the atmosphere. *Phys. Chem. Chem. Phys.* 13 (43), 19238. doi:10.1039/c1cp22617g

Krieger, U. K., Marcolli, C., and Reid, J. P. (2012). Exploring the complexity of aerosol particle properties and processes using single particle techniques. *Chem. Soc. Rev.* 41 (19), 6631. doi:10.1039/c2cs35082c

Kucinski, T. M., Dawson, J. N., and Freedman, M. A. (2019). Size-Dependent liquid-liquid phase separation in atmospherically relevant complex systems. *J. Phys. Chem. Lett.* 10 (21), 6915–6920. doi:10.1021/acs.jpclett.9b02532

Ladino, L. A., Zhou, S., Yakobi-Hancock, J. D., Aljawhary, D., and Abbatt, J. P. D. (2014). Factors controlling the ice nucleating abilities of α-pinene SOA particles. *J. Geophys. Res. Atmos.* 119 (14), 9041–9051. doi:10.1002/2014jd021578

Lee, S.-W., Chon, J., Kim, S.-B., and Kim, E. J. (2017). Network potential analysis among agricultural villages based on landscape resources-focused on dangjin, seosan, and taean in chungchungnam-do region. *J. Korean Soc. Rural. Plan.* 23 (3), 1–12. doi:10.7851/ksrp.2017.23.3.001

Li, J., Forrester, S. M., and Knopf, D. A. (2020). Heterogeneous oxidation of amorphous organic aerosol surrogates by O_3, NO_3, and OH at typical tropospheric temperatures. *Atmos. Chem. Phys.* 20 (10), 6055–6080. doi:10.5194/acp-20-6055-2020

Lilek, J., and Zuend, A. (2022). A predictive viscosity model for aqueous electrolytes and mixed organic-inorganic aerosol phases. *Atmos. Chem. Phys.* 22 (5), 3203–3233. doi:10.5194/acp-22-3203-2022

Liu, Y. C., Wu, Z. J., Wang, Y., Xiao, Y., Gu, F. T., Zheng, J., et al. (2017). Submicrometer particles are in the liquid state during heavy haze episodes in the urban atmosphere of beijing, China. *Environ. Sci. Technol. Lett.* 4 (10), 427–432. doi:10.1021/acs.estlett.7b00352

Murray, B. J., Haddrell, A. E., Peppe, S., Davies, J. F., Reid, J. P., O'Sullivan, D., et al. (2012). Glass formation and unusual hygroscopic growth of iodic acid solution droplets with relevance for iodine mediated particle formation in the marine boundary layer. *Atmos. Chem. Phys.* 12 (18), 8575–8587. doi:10.5194/acp-12-8575-2012

Pajunoja, A., Hu, W. W., Leong, Y. J., Taylor, N. F., Miettinen, P., Palm, B. B., et al. (2016). Phase state of ambient aerosol linked with water uptake and chemical aging in the southeastern US. *Atmos. Chem. Phys.* 16 (17), 11163–11176. doi:10.5194/acp-16-11163-2016

Park, S., Son, S.-C., and Lee, K.-Y. (2022). Chemical characteristics of $PM_{2.5}$ during spring and fall at two sites in Chungcheongnam-do, South Korea; insight into Fe solubility and SO_4^{2-} formation. *Atmos. Pollut. Res.* 13 (3), 101350. doi:10.1016/j.apr.2022.101350

Peng, J., Hu, M., Guo, S., Du, Z., Zheng, J., Shang, D., et al. (2016). Markedly enhanced absorption and direct radiative forcing of black carbon under polluted urban environments. *Proc. Natl. Acad. Sci. U. S. A.* 113 (16), 4266–4271. doi:10.1073/pnas.1602310113

Pöhlker, C., Wiedemann Kenia, T., Sinha, B., Shiraiwa, M., Gunthe Sachin, S., Smith, M., et al. (2012). Biogenic potassium salt particles as seeds for secondary organic aerosol in the Amazon. *Science* 337 (6098), 1075–1078. doi:10.1126/science.1223264

Pörtner, H., Roberts, D., Masson-Delmotte, V., Zhai, P., Tignor, M., Poloczanska, E., et al. (2019). *IPCC special report on the ocean and cryosphere in a changing climate*. Geneva, Switzerland: IPCC Intergovernmental Panel on Climate Change.

Reid, J. P., Bertram, A. K., Topping, D. O., Laskin, A., Martin, S. T., Petters, M. D., et al. (2018). The viscosity of atmospherically relevant organic particles. *Nat. Commun.* 9 (1), 956. doi:10.1038/s41467-018-03027-z

Renbaum-Wolff, L., Grayson, J. W., Bateman, A. P., Kuwata, M., Sellier, M., Murray, B. J., et al. (2013). Viscosity of alpha-pinene secondary organic material and implications for particle growth and reactivity. *Proc. Natl. Acad. Sci. U. S. A.* 110 (20), 8014–8019. doi:10.1073/pnas.1219548110

Renbaum-Wolff, L., Song, M., Marcolli, C., Zhang, Y., Liu, P. F., Grayson, J. W., et al. (2016). Observations and implications of liquid–liquid phase separation at high relative humidities in secondary organic material produced by α-pinene ozonolysis without inorganic salts. *Atmos. Chem. Phys.* 16 (12), 7969–7979. doi:10.5194/acp-16-7969-2016

Riemer, N., Vogel, H., Vogel, B., Anttila, T., Kiendler-Scharr, A., Mentel, T. F., et al. (2009). Relative importance of organic coatings for the heterogeneous hydrolysis of N_2O_5 during summer in Europe. *J. Geophys. Res.* 114 (D17), D17307. doi:10.1029/2008jd011369

Riemer, N., Ault, A. P., West, M., Craig, R. L., and Curtis, J. H. (2019). Aerosol mixing state: Measurements, modeling, and impacts. *Rev. Geophys.* 57 (2), 187–249. doi:10.1029/2018rg000615

Sauerwein, M., and Chan, C. K. (2017). Heterogeneous uptake of ammonia and dimethylamine into sulfuric and oxalic acid particles. *Atmos. Chem. Phys.* 17 (10), 6323–6339. doi:10.5194/acp-17-6323-2017

Schmedding, R., Rasool, Q. Z., Zhang, Y., Pye, H. O. T., Zhang, H., Chen, Y., et al. (2020). Predicting secondary organic aerosol phase state and viscosity and its effect

on multiphase chemistry in a regional-scale air quality model. *Atmos. Chem. Phys.* 20 (12), 8201–8225. doi:10.5194/acp-20-8201-2020

Seinfeld, J. H., and Pandis, S. N. (2016). *Atmospheric chemistry and physics: From air pollution to climate change,*. 3rd Edn. Hoboken, NJ: John Wiley & Sons.

Shiraiwa, M., and Seinfeld, J. H. (2012). Equilibration timescale of atmospheric secondary organic aerosol partitioning. *Geophys. Res. Lett.* 39 (24), 2012GL054008. doi:10.1029/2012gl054008

Shiraiwa, M., Yee, L. D., Schilling, K. A., Loza, C. L., Craven, J. S., Zuend, A., et al. (2013). Size distribution dynamics reveal particle-phase chemistry in organic aerosol formation. *Proc. Natl. Acad. Sci. U. S. A.* 110 (29), 11746–11750. doi:10.1073/pnas.1307501110

Song, M., Marcolli, C., Krieger, U. K., Zuend, A., and Peter, T. (2012a). Liquid-liquid phase separation and morphology of internally mixed dicarboxylic acids/ammonium sulfate/water particles. *Atmos. Chem. Phys.* 12 (5), 2691–2712. doi:10.5194/acp-12-2691-2012

Song, M., Marcolli, C., Krieger, U. K., Zuend, A., and Peter, T. (2012b). Liquid-liquid phase separation in aerosol particles: Dependence on O:C, organic functionalities, and compositional complexity. *Geophys. Res. Lett.* 39 (19), L19801. doi:10.1029/2012GL052807

Song, M., Marcolli, C., Krieger, U. K., Lienhard, D. M., and Peter, T. (2013). Morphologies of mixed organic/inorganic/aqueous aerosol droplets. *Faraday Discuss.* 165, 289. doi:10.1039/c3fd00049d

Song, M., Liu, P. F., Hanna, S. J., Li, Y. J., Martin, S. T., Bertram, A. K., et al. (2015). Relative humidity-dependent viscosities of isoprene-derived secondary organic material and atmospheric implications for isoprene-dominant forests. *Atmos. Chem. Phys.* 15 (9), 5145–5159. doi:10.5194/acp-15-5145-2015

Song, M. J., Liu, P. F., Hanna, S. J., Zaveri, R. A., Potter, K., You, Y., et al. (2016). Relative humidity-dependent viscosity of secondary organic material from toluene photo-oxidation and possible implications for organic particulate matter over megacities. *Atmos. Chem. Phys.* 16 (14), 8817–8830. doi:10.5194/acp-16-8817-2016

Song, M. J., Liu, P. F., Martin, S. T., and Bertram, A. K. (2017). Liquid-liquid phase separation in particles containing secondary organic material free of inorganic salts. *Atmos. Chem. Phys.* 17 (18), 11261–11271. doi:10.5194/acp-17-11261-2017

Song, M., Maclean, A. M., Huang, Y. Z., Smith, N. R., Blair, S. L., Laskin, J., et al. (2019). Liquid-liquid phase separation and viscosity within secondary organic aerosol generated from diesel fuel vapors. *Atmos. Chem. Phys.* 19 (19), 12515–12529. doi:10.5194/acp-19-12515-2019

Song, Y. C., Lilek, J., Lee, J. B., Chan, M. N., Wu, Z. J., Zuend, A., et al. (2021). Viscosity and phase state of aerosol particles consisting of sucrose mixed with inorganic salts. *Atmos. Chem. Phys.* 21 (13), 10215–10228. doi:10.5194/acp-21-10215-2021

Su, H., Cheng, Y., and Poschl, U. (2020). New multiphase chemical processes influencing atmospheric aerosols, air quality, and climate in the anthropocene. *Acc. Chem. Res.* 53 (10), 2034–2043. doi:10.1021/acs.accounts.0c00246

Ting, Y.-C., Young, L.-H., Lin, T.-H., Tsay, S.-C., Chang, K.-E., Hsiao, T.-C., et al. (2022). Quantifying the impacts of PM2. 5 constituents and relative humidity on visibility impairment in a suburban area of eastern Asia using long-term *in-situ* measurements. *Sci. Total Environ.* 818, 151759. doi:10.1016/j.scitotenv.2021.151759

Vester, B. P., Ebert, M., Barnert, E. B., Schneider, J., Kandler, K., Schutz, L., et al. (2007). Composition and mixing state of the urban background aerosol in the Rhein-Main area (Germany). *Atmos. Environ. X.* 41 (29), 6102–6115. doi:10.1016/j.atmosenv.2007.04.021

Virtanen, A., Joutsensaari, J., Koop, T., Kannosto, J., Yli-Pirilä, P., Leskinen, J., et al. (2010). An amorphous solid state of biogenic secondary organic aerosol particles. *Nature* 467 (7317), 824–827. doi:10.1038/nature09455

Wang, G., Zhang, R., Gomez, M. E., Yang, L., Levy Zamora, M., Hu, M., et al. (2016). Persistent sulfate formation from London Fog to Chinese haze. *Proc. Natl. Acad. Sci. U. S. A.* 113 (48), 13630–13635. doi:10.1073/pnas.1616540113

Wang, L.-N., Cai, C., and Zhang, Y.-H. (2017). Kinetically determined hygroscopicity and efflorescence of sucrose–ammonium sulfate aerosol droplets under lower relative humidity. *J. Phys. Chem. B* 121 (36), 8551–8557. doi:10.1021/acs.jpcb.7b05551

Winston, P. W., and Bates, D. H. (1960). Saturated solutions for the control of humidity in biological-research. *Ecology* 41(1), 232–237. doi:10.2307/1931961

World Health Organization (2021). *WHO global air quality guidelines: Particulate matter ($PM_{2.5}$ and PM_{10}), ozone, nitrogen dioxide, sulfur dioxide and carbon monoxide*. World Health Organization. Available online at: https://apps.who.int/iris/handle/10665/345329.

Xu, R. S., Lam, H. K., Wilson, K. R., Davie, J. F., Son, M. J., Li, W. T., et al. (2020). Effect of inorganic-to-organic mass ratio on the heterogeneous OH reaction rates of erythritol: Implications for atmospheric chemical stability of 2-methyltetrols. *Atmos. Chem. Phys.* 20 (6), 3879–3893. doi:10.5194/acp-20-3879-2020

Ye, Q., Gu, P., Li, H. Z., Robinson, E. S., Lipsky, E., Kaltsonoudis, C., et al. (2018). Spatial variability of sources and mixing state of atmospheric particles in a metropolitan area. *Environ. Sci. Technol.* 52 (12), 6807–6815. doi:10.1021/acs.est.8b01011

Yli-Juuti, T., Pajunoja, A., Tikkanen, O. P., Buchholz, A., Faiola, C., Vaisanen, O., et al. (2017). Factors controlling the evaporation of secondary organic aerosol from alpha-pinene ozonolysis. *Geophys. Res. Lett.* 44 (5), 2562–2570. doi:10.1002/2016GL072364

You, Y., Renbaum-Wolff, L., Carreras-Sospedra, M., Hanna, S. J., Hiranuma, N., Kamal, S., et al. (2012). Images reveal that atmospheric particles can undergo liquid-liquid phase separations. *Proc. Natl. Acad. Sci. U. S. A.* 109 (33), 13188–13193. doi:10.1073/pnas.1206414109

You, Y., Smith, M. L., Song, M. J., Martin, S. T., and Bertram, A. K. (2014). Liquid-liquid phase separation in atmospherically relevant particles consisting of organic species and inorganic salts. *Int. Rev. Phys. Chem.* 33 (1), 43–77. doi:10.1080/0144235x.2014.890786

Zelenyuk, A., Cai, Y., and Imre, D. (2006). From agglomerates of spheres to irregularly shaped particles: Determination of dynamic shape factors from measurements of mobility and vacuum aerodynamic diameters. *Aerosol Sci. Technol.* 40 (3), 197–217. doi:10.1080/02786820500529406

Zhang, Y., Tang, L., Croteau, P. L., Favez, O., Sun, Y., Canagaratna, M. R., et al. (2017). Field characterization of the $PM_{2.5}$ aerosol chemical speciation monitor: Insights into the composition, sources, and processes of fine particles in eastern China. *Atmos. Chem. Phys.* 17 (23), 14501–14517. doi:10.5194/acp-17-14501-2017